



# SYMBOLIC MODELING OF ROBOTIC MANIPULATORS

A.A.N. Aljawi<sup>1</sup>, A.S. Balamesh<sup>1</sup>, T. D. Almatrafi<sup>2</sup> and M. Akyurt<sup>1</sup>

1: College of Engineering, King Abdulaziz University, P.O. Box 80204, Jeddah 21589

2: Saudi Electricity Company, Power Station, Madinah Al-Munawwarah.

E-mail: akyurt99@yahoo.com

## ABSTRACT

Forward and inverse kinematic modeling of robotic manipulators is discussed. Details are given for the forward kinematic analysis of the KAU articulated robot (RPR version) as well as the inverse kinematic analysis of the same. Solutions for prismatic and revolute joints are affected by the use of MapleV.

**Keywords:** arm, forward, inverse, kinematic modeling, manipulator, robot.

)

(

Maple V.

## 1. INTRODUCTION

A robotic manipulator (arm) consists of a chain of links interconnected by joints. There are typically two types of joints; *revolute* joint (rotation joint) and *prismatic* joint (sliding). It would be desirable to control both the position and orientation of a tool or workpiece, located at the tip of the manipulator, in its three-dimensional workspace. The tool can be programmed to follow a planned trajectory, provided relationships between joint variables and the position and the orientation of the tool are formulated. This task is called the *direct kinematics problem*.

## 2. FORWARD KINEMATIC ANALYSIS

A robotic arm can be modeled as a chain of rigid links interconnected by revolute and prismatic joints. A general arm equation that represents the kinematic motion of the manipulator can be obtained by systematically assigning coordinate frames for each link. Figure 1 shows that the relative position and orientation for each adjacent pair of links that is

connected by either a revolute or a prismatic joint can be specified by two joint parameters where joint  $k$  connects link  $k-1$  to link  $k$ . The parameters associated with joint  $k$  are defined with respect to  $\mathbf{z}^{k-1}$ , that is aligned with the axis of joint  $k$ . The first joint parameter  $\theta_k$ , is called the joint angle. It is the rotation about  $\mathbf{z}^{k-1}$  needed to make  $\mathbf{x}^{k-1}$  parallel to  $\mathbf{x}^k$ . The second joint parameter,  $\mathbf{d}^k$  is called the joint distance. It is the translation along  $\mathbf{z}^{k-1}$  needed to make  $\mathbf{x}^{k-1}$  intersect with  $\mathbf{x}^k$ . Note that for each joint, it will always be the case that one of these parameters is fixed and the other is variable. As indicated in Table 1, the variable joint parameter depends on the type of joint. For instance, for a revolute joint, the joint angle  $\theta_k$  is variable while the joint distance  $\mathbf{d}^k$  is fixed while for a prismatic joint, the joint distance  $\mathbf{d}^k$  is variable and the joint angle  $\theta_k$  is fixed.

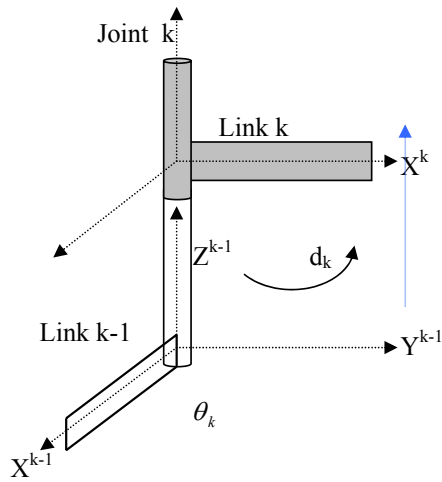


Fig. 1 Joint angle  $\theta$  and joint distance  $d$ .

Table 1 Kinematic Parameters

Arm Parameter	Symbol	Revolute joint (R)	Prismatic Joint (P)
Joint Angle	$\theta$	Variable	Fixed
Joint Distance	$d$	Fixed	Variable
Link Length	$a$	Fixed	Fixed
Link Twist Angle	$\alpha$	Fixed	Fixed

Since there is a joint between adjacent links, there is also a link between successive joints. Figure 2 shows that the relative position and orientation of the axes of two successive joints can be specified by, two link parameters. Link  $k$  connects joint  $k$  to joint  $k+1$ . The parameters associated with link  $k$  are defined with respect to  $\mathbf{x}^k$ , which is a common normal between the axes of joint  $k$  and joint  $k+1$ . The first link parameter,  $a_k$  is called link length. It is the

translation along  $x^k$  needed to make the axis  $z^{k-1}$  intersect with axis  $Z^k$ . The second link parameter,  $\alpha_k$  is called the twist angle. It is the rotation about the  $x$  axis needed to make axis  $z_{k-1}$  parallel with  $z_k$ . These parameters are always constants and are specified as part of the mechanical design.

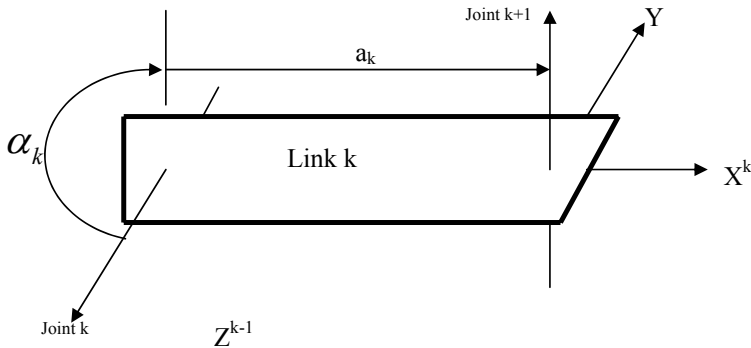


Fig. 2 Link length  $a$  and link twist angle  $\alpha$

For industrial robots, the link twist angle is usually a multiple of  $\pi/2$  radians. Sometimes the axes of joint  $k$  and  $k-1$  intersect, in which case the length of link  $k$  is zero. Links of length zero occur in robots with spherical wrists where the last  $n-3$  axes intersect ( $n$  is the number of degrees of freedom). For an  $n$ -axis robotic manipulator, the  $4n$  kinematic parameters constitute the minimal set needed to specify the kinematic configuration of the robot. For each axis, three of the parameters are fixed and depend on the mechanical design, while the fourth parameter is the joint variable, as stated in Table 1. For a Cartesian robot, the first three joint variables are all joint distances, whereas for an articulated robot, the first three joint variables are all angles. Between these two extremes lie the cylindrical and spherical robots.

Once a set of link coordinates is assigned using the D-H algorithm [Denavit and Hartenberg, 1955], one can then transform coordinate frame  $k$  to coordinate  $k-1$  using a homogeneous coordinate transformation matrix called the arm matrix [Dehlawi, et al., 1996].

$$T_{k-1}^k = \begin{bmatrix} C\theta_k & -C\alpha_k S\theta_k & S\alpha_k S\theta_k & a_k C\theta_k \\ S\theta_k & C\alpha_k C\theta_k & -S\alpha_k C\theta_k & a_k S\theta_k \\ 0 & S\alpha_k & C\alpha_k & d_k \\ 0 & 0 & 0 & 1 \end{bmatrix}$$

The inverse of this transformation matrix can be found to be:

$$T_K^{K-1} = \begin{bmatrix} C\theta_K & S\theta_K & 0 & -a_k \\ -C\alpha_K S\theta_K & C\alpha_K C\theta_K & S\alpha_K & -d_k S\alpha_K \\ S\alpha_K S\theta_K & -S\alpha_K C\theta_K & C\alpha_K & -d_k C\alpha_K \\ 0 & 0 & 0 & 1 \end{bmatrix}$$

When considering a six-degree-of-freedom manipulator, the total equation is composed of the arm motion and the wrist motion that comprises the **Euler** angles or roll-pitch-yaw angles.

$$\text{Arm motion} = T_{\text{base}}^{\text{wrist}}(\theta_1, \theta_2, \theta_3) = T_0^1(\theta_1) T_1^2(\theta_2) T_2^3(\theta_3) = T_0^3$$

Where,  $T_0^3$  is the orientation and position of the arm with respect to the base coordinate frame.

$$\text{Wrist motion} = T_{\text{wrist}}^{\text{tool}}(\theta_4, \theta_5, \theta_6) = T_3^4(\theta_4) T_4^5(\theta_5) T_5^6(\theta_6) = T_3^6$$

and  $T_3^6$  is the orientation and position of the grip of the wrist with respect to the third link coordinate frame. Note that  $T_5^6(\theta_6)$  maps tool-tip coordinates into roll coordinates,  $T_4^5(\theta_5)$  maps roll coordinates into pitch coordinates, and  $T_3^4(\theta_4)$  maps pitch coordinates into wrist yaw coordinates. Thus the composite transformation  $T_3^6(\theta_4, \theta_5, \theta_6)$  maps tool-tip coordinates into wrist coordinates. Similarly  $T_2^3(\theta_3)$  maps wrist coordinates into elbow coordinates,  $T_1^2(\theta_2)$  maps elbow coordinates into shoulder coordinates, and  $T_0^1(\theta_1)$  maps shoulder coordinates into base coordinates. Thus the composite transformation  $T_3^6(\theta_4, \theta_5, \theta_6)$  maps tool-tip coordinates into wrist coordinates. The general solution can be expressed as:

$$[\text{Total motion}] = [\text{arm motion}][\text{wrist motion}]$$

Using the D-H method (algorithm), the end-effector position can be written as:

$$T_{\text{base}}^{\text{tool}}(\theta_1, \theta_2, \theta_3, \theta_4, \theta_5, \theta_6) = T_0^1(\theta_1) T_1^2(\theta_2) T_2^3(\theta_3) T_3^4(\theta_4) T_4^5(\theta_5) T_5^6(\theta_6)$$

Note that the  $T_{\text{base}}^{\text{tool}} = T_0^6$  given for the end-effector can be written as a 4 x 4 homogeneous matrix composed of an orientation submatrix **R** and a position matrix as:

$$T_{\text{base}}^{\text{wrist}} = \left[ \begin{array}{ccc|c} & & & \\ & \mathbf{R} & & \mathbf{P} \\ \hline 0 & 0 & 0 & 1 \end{array} \right]$$

Thus, in the direct kinematic solution, for any given value of the joint angles  $\theta$ , the arm matrix  $T_{base}^{tool}$  can be evaluated. The upper left 3x3 matrix,  $\mathbf{R}$ , specifies the orientation of the tool, while the 3 x 1 upper right submatrix  $\mathbf{P}$  specifies the position of the tool-tip.

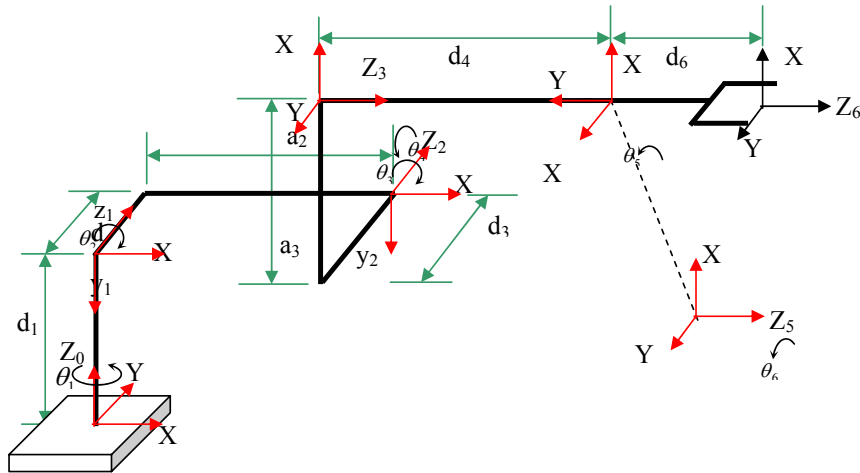


Fig.3 Link coordinate diagram of the six-axis KAU robot



Fig. 4 The KAU robot in the machine shop [Dehlawi, et al., 1996].

Below, due to space restrictions, we present a detailed kinematic analysis for only the RPR (roll-pitch-roll) version of the KAU robot (Figs. 3 and 4). Analyses of Cartesian, cylindrical and spherical robots as well as for the PYR type of KAU articulated robot are presented elsewhere [Dehlawi, et al., 1996; Al-Matrafi, 2000].

For ease of discussion, and to unify the parameters for the link height and length for the considered cases, we set the height of link 1 from the base as  $h_1$ , the length and offset of the

axis of rotation of link 2 from link 1 as  $l_1$  and  $e_2$ , respectively; the length and offset of the axis of rotation of link3 from link 2 as  $l_2$  and  $e_2$ , respectively; the offset of the axes of rotation of the wrist from link 3 as  $h_2$ , and finally the distance from the tool-tip to the base of the wrist axis of rotation as  $l_3$ . Thus, using the above parameters, the values for the  $a$ 's and  $d$ 's for the two cases shown in Fig. 3 become  $d_1=h_1, d_2=e_1, a_2=l_1, d_3=-e_2, a_3=h_2, d_4=l_2, d_6=l_3$ . Then, following the D-H algorithm, the kinematic parameters are defined and shown in Table 2.5.

Table 2.5, The kinematic parameters of RPR robot.

Axis	$\theta$	d	A	$\alpha$	Home
1	$\theta_1$	$h_1$	0	0	0
2	$\theta_2$	$e_1$	$l_1$	0	$\pi/2$
3	$\theta_3$	$-e_2$	$h_2$	$-\pi/2$	0
4	$\theta_4$	$l_2$	0	0	$\pi/2$
5	$\theta_5$	0	0	0	$\pi/2$
6	$\theta_6$	$l_3$	0	0	0

The Maple V computer package for symbolic math was used to generate the arm matrices. It may be shown [Al-Matrafi, 2000] that the matrix operation from base to wrist  $T_b^w$  and from wrist to tool  $T_w^t$  can be stated in a simplified form as:

$$T_b^w = \begin{bmatrix} C_1 C_{23} & S_1 & -C_1 S_{23} & C_1(h_2 C_{23} + l_1 C_2) - S_1(e_1 - e_2) \\ S_1 C_{23} & C_1 & -S_1 S_{23} & S_1(h_2 C_{23} + l_1 C_2) + C_1(e_1 - e_2) \\ -S_{23} & 0 & -C_{23} & -h_2 S_{23} - l_1 S_2 + h_1 \\ 0 & 0 & 0 & 1 \end{bmatrix} \quad (2-10)$$

$$T_w^t = \begin{bmatrix} C_4 C_5 C_6 - S_4 S_6 & -C_4 C_5 S_6 - S_4 C_6 & C_4 S_5 & l_3 C_4 S_5 \\ S_4 C_5 C_6 + C_4 S_6 & -S_4 C_5 S_6 + C_4 C_6 & S_4 S_5 & l_3 S_4 S_5 \\ -S_5 C_6 & S_6 S_5 & C_5 & l_3 C_5 + l_2 \\ 0 & 0 & 0 & 1 \end{bmatrix} \quad (2-11)$$

Where  $C_{ij} = \cos(\theta_i + \theta_j)$  and  $S_{ij} = \sin(\theta_i + \theta_j)$

Now using the home position angles defined in Table 2.5 and using Maple V, the orientation and position of the tool-tip matrices, T' can be given as:

$$T_b^w = \begin{bmatrix} 0 & 0 & 1 & l_1 + l_2 + l_3 \\ 0 & -1 & 0 & e_1 - e_2 \\ 1 & 0 & 0 & h_1 + h_2 \\ 0 & 0 & 0 & 1 \end{bmatrix}$$

The analysis of the forward kinematics problem presented above was done by using the analytical method. The analytical method gives many solutions for the forward problem, but difficulty is faced when one starts to determine robot arm parameters by using the D-H algorithm. The mathematical program (MapleV) was used to solve the forward kinematics problem after the robot arm equations were described in the form of matrices. We use these equations in what follows to find the solutions to the inverse kinematics problem.

### 3. INVERSE KINEMATIC ANALYSIS

The inverse kinematics problem is concerned with finding the joint coordinates, given the coordinates of the tool tip with respect to the base of the robot. This is needed, because what we can directly control, through the actuators, are the joint coordinates. So, to position the tool tip at a particular location, the joint coordinates are found through inverse kinematics, and then each joint is moved as dictated by its coordinates.

Since both the desired position and orientation of the end-effector need to be controlled, the inverse kinematics solution is more practical significance than the direct solution. The inverse kinematics problem is more difficult than the direct kinematics problem because a systematic closed-form solution applicable to robots in general is not available [Dehlawi, et al., 1996]. Moreover, when closed-form solutions to the arm equation can be found, they are seldom-unique [Schilling, 1990].

In general, the inverse kinematics problem can be solved by various methods such as inverse transform [Paul, 1981], screw algebra and dual matrices [Denavit and Hartenberg, 1955], dual quaternion [Yang and Frnden, 1964], iteratively [Uicker, et al., 1964], and by the use of geometric approaches [Lee and Ziegler, 1983].

Pieper in 1968 presented the kinematic solution for any 6-degree of freedom manipulator which has revolute or prismatic pairs for the first three joints, and where the joint axes of the last three joints intersect at a point. The solution can be expressed as a fourth-degree polynomial in one unknown, and closed for solution for the remaining unknowns. Paul [1981] presented an inverse transform technique using 4x4 homogeneous transformation matrices in solving the kinematic solution for the same class of simple manipulators as discussed by Pieper. Although the resulting solution is correct, this method suffers from the fact that the

solution does not give a clear indication as how to select an appropriate solution from among several possible solutions for a particular arm configuration [Fu, 1987].

The key to the solution of the direct kinematics problem outlined above is the (D-H) algorithm, which is a systematic procedure for assigning link coordinates to a robotic manipulator. Successive transformations between adjacent coordinate frames, starting at the tool tip and working back to the base of the robot, then lead to the arm matrix. The arm matrix represents positions  $P$  and orientation  $R$  of the tool in the base frame as a function of joint variables  $q$ , as shown in Fig. 5.

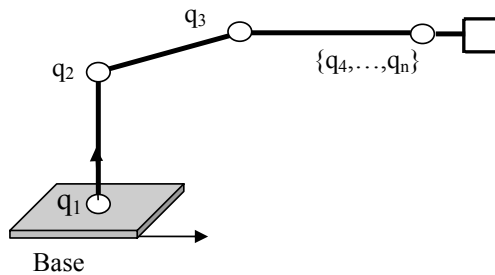


Fig. 5 Tool configuration as a function of joint variables.

The inverse kinematics problem is more difficult than the direct kinematics problem because no single explicit systematic procedure analogous to the D-H algorithm is available. As a result, each robot or generically similar class of robots has to be treated separately. The solution to the inverse kinematics problem is, however, much more useful.

The inverse kinematics problem is defined as follows: Given a position  $P=(x,y,z)$  and orientation  $R=[r^1 \ r^2 \ r^3]$  for the tool, where vectors  $r^1, r^2$  and  $r^3$  represent the tool normal, sliding and approach vectors, respectively, the inverse kinematics problem is concerned with finding the values of joint variables  $q$  or  $\theta$  which satisfy the arm equation [Dehlawi, et al., 1996].

There are certain characteristics of the solution that hold in general. Thus, if the desired tool-tip position is outside the robot's work envelope, then no solution can exist. Furthermore, even when  $P$  is within the work envelope, there may be certain tool orientations  $R$  which are not realizable without violating one or more of the joint variable limits. Indeed, if the robot has fewer than three degrees of freedom to orient the tool, then whole classes of orientations are unrealizable [Schilling, 1990].



The inverse kinematics problem can be decomposed into two smaller sub-problems by partitioning the original problem at the wrist. Given the tool tip position  $\mathbf{P}$  and tool orientation  $\mathbf{R}$ , the *wrist position*  $P^{wrist}$  can be inferred from  $P$  by working backward along the approach vector:

$$P^{wrist} = P - d_n r^3 \quad (3-1)$$

Here the joint distance  $d_n$  represents the tool length for an  $n$ -axis robot as long as the last axis is a tool roll axis. The approach vector  $r^3$  is simply the third column of the rotation matrix  $\mathbf{R}$ . Once the wrist position  $P^{wrist}$  is obtained from  $\{P, \mathbf{R}, d_n\}$ , the first three joint variables  $\{q_1, q_2, q_3\}$  that are used to position the wrist can be obtained from the following *reduced arm equation*:

$$T_{base}^{wrist}(q_1, q_2, q_3) = \begin{bmatrix} p - d_n r^3 \\ 1 \end{bmatrix} \quad (3-2)$$

The fourth column of  $T_{base}^{wrist}$  represents the homogeneous coordinates of the origin of the wrist frame  $L_3$  relative to the base frame  $L_0$ . Since wrist coordinates depend only on joint variables  $\{q_1, q_2, q_3\}$ , these joint variables of the major axes can be solved for *separately* using Eq. (3-2). Once the major axis variables  $\{q_1, q_2, q_3\}$  are found, their values can then be substituted into the general arm equation in Eq.(3-3), and it can be solved for the remaining tool orientation variables  $\{q_4, \dots, q_n\}$  [Schilling, 1990].

$$T_{wrist}^{tool} = \begin{bmatrix} R_{11} & R_{12} & R_{13} & p_1 \\ R_{21} & R_{22} & R_{23} & p_2 \\ R_{31} & R_{32} & R_{33} & p_3 \\ 0 & 0 & 0 & 1 \end{bmatrix} \quad (3-3)$$

The existence of a solution to the inverse kinematics problem is not the only issue that needs to be addressed. When solutions do exist, typically they are not unique [Schilling, 1990]. Indeed, multiple solutions can arise in a number of ways. For example, some robots are designed with  $n$  axes where  $n > 6$ . For these robots, infinitely many solutions to the inverse kinematics problem typically exist. We refer to robots with more than six axes as *kinematically redundant* robots, because they have more degrees of freedom than are necessary to establish arbitrary tool configurations. These extra degrees of freedom add flexibility to the manipulator. For example, a redundant robot might be commanded to reach around an obstacle and manipulate an otherwise inaccessible object. Here some of the degrees of freedom can be used to avoid the obstacle while the remaining degrees of freedom are used to configure the tool.

Even when a robot is not kinematically redundant there are often circumstances in which the solution to the inverse kinematics problem is not unique. Several distinct solutions can arise when the size of the joint-space work envelope  $Q$  is sufficiently large. As a case in point, consider the articulated-coordinate robot shown in Fig. 6. If the limits on the range of travel for the shoulder, elbow, and tool pitch joints are sufficiently large, then two distinct solutions exist for the simple task of placing the tool out in front of the robot.

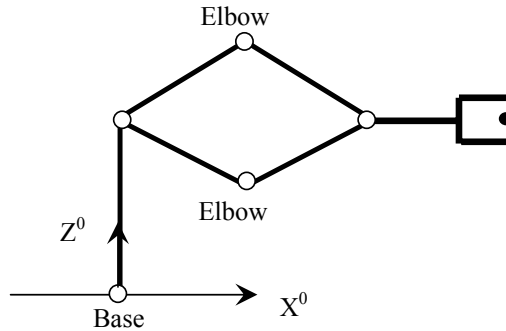


Fig. 6 Multiple solutions with a non-redundant robot.

Figure 6 refers to the two solutions characterized by the *elbow-up* and the *elbow-down* configurations. In tool-configuration space the two solutions are identical, because they produce the same  $\mathbf{P}$  and  $\mathbf{R}$ , but in joint space they are clearly distinct. Typically the elbow-up solution is preferred, because it reduces the chance of a collision between the links of the arm and obstacles resting on the work surface.

The solution to the inverse kinematics problem can be approached either numerically or analytically. In the present work the analytical method is preferred since it is faster than the numerically approximation method, and it can be used to identify multiple solutions. Using the analytical approach, the specific nature of the direct kinematic equations is considered while determining a closed-form expression for the solution.

The analytical solution technique was applied to determine the inverse kinematic solution of a number of different types of robots [Dehlawi, et al., 1996; Al-Matrafi, 2000]. Below, due to space restrictions, we present the analysis for only the RPR version of the KAU robot (Figs. 3 and 4). Analyses of Cartesian, cylindrical and spherical robots as well as for the PYR type of KAU articulated robot are presented elsewhere [Dehlawi, et al., 1996; Al-Matrafi, 2000].

It may be shown, by the use of the relation

$$P^{wrist} = P - d_n r^3$$

that the position of the wrist is given by

$$P_x = C_1[-l_2 S_{23} + h_2 C_{23} + l_1 C_2] - (e_1 - e_2) S_1,$$

$$P_y = S_1[-l_2 S_{23} + h_2 C_{23} + l_1 C_2] + (e_1 - e_2) C_1,$$

and

$$P_z = -l_2 C_{23} - h_2 S_{23} - l_1 S_2 + h_1$$

### 3.1 Solution for $\theta_1$

From the above equations it follows that,

$$P_y \cos \theta_1 - P_x \sin \theta_1 = e_1 - e_2$$

Solving for  $\theta_1$ , one finds

$$\theta_1 = 2 \arctan \left[ \frac{-P_x \pm \sqrt{P_x^2 + P_y^2 - (e_1 - e_2)^2}}{P_y + e_1 - e_2} \right],$$

Where the  $-$  and  $+$  signs represent the right and left arm solutions, respectively. It should be noted that the above solution lies in the  $(-\pi, \pi)$  interval, and there is no need to use the atan2 function.

### 3.2 Solution for $\theta_2$ and $\theta_3$

New quantities are defined as follows:

$$P'_x = P_x + (e_1 - e_2) S_1$$

$$P'_y = P_y - (e_1 - e_2) C_1$$

$$P'_z = P_z - h_1$$

and

$$b = P'_x C_1 + P'_y S_1$$

Then, it follows that

$$P'_x = C_1[-l_2 S_{23} + h_2 C_{23} + l_1 C_2]$$

$$P'_z = S_1[-l_2 S_{23} + h_2 C_{23} + l_1 C_2]$$

$$P'_z = -l_2 C_{23} - h_2 S_{23} - l_1 S_2$$

and

$$b = -l_2 S_{23} + h_2 C_{23} + l_1 C_2$$

Now,

$$b^2 + P_z'^2 = h_2^2 + l_1^2 + l_2^2 - 2l_1 l_2 \sin \theta_3 + 2l_1 h_2 \cos \theta_3$$

or

$$h_2 \cos \theta_3 - l_2 \sin \theta_3 = \frac{b^2 + P_z'^2 - h_2^2 - l_1^2 - l_2^2}{2l_1}$$

Also, may be observed that

$$\begin{aligned} b \cos \theta_2 - P_z' \sin \theta_2 &= h_2 \cos \theta_3 - l_2 \sin \theta_3 + l_1 \\ &= \frac{b^2 + P_z'^2 - h_2^2 - l_1^2 - l_2^2}{2l_1} + l_1 \\ &= u \end{aligned}$$

where

$$u = \frac{b^2 + P_z'^2 - h_2^2 - l_1^2 - l_2^2}{2l_1}$$

Solving for  $\theta_2$  yields:

$$\theta_2 = 2 \arctan \left[ \frac{-P_z' \pm \sqrt{P_z'^2 + b^2 - u^2}}{b + u} \right]$$

Where the – and + signs represent the above and below elbow solutions, respectively, in case of right arm solution and vise versa.

Similarly

$$-l_2 \cos \theta_3 - h_2 \sin \theta_3 = P_z' \cos \theta_2 + b \sin \theta_2$$

Which together with the equation

$$h_2 \cos \theta_3 - l_2 \sin \theta_3 = b \cos \theta_2 - P_z' \sin \theta_2 - l_1$$

form a set of two equations in two unknowns, since  $\theta_2$  is already known. Thus, the solution for  $\theta_3$  becomes:

$$\cos \theta_3 = \frac{(h_2 b - l_2 P_z') \cos \theta_2 - (h_2 P_z' + l_2 b) \sin \theta_2 - l_1 h_2}{l_2^2 + h_2^2}$$

$$\sin \theta_3 = \frac{-(h_2 P'_z + l_2 b) \cos \theta_2 - (h_2 b - l_2 P'_z) \sin \theta_2 + l_1 l_2}{l_2^2 + h_2^2}$$

and

$$\theta_3 = \text{atan2}(\sin \theta_3, \cos \theta_3)$$

### 3.3 The solution of the last three joints

It is possible to obtain the following equations from the forward kinematics problem:

$$R_{11} = C_1 C_{23} C_4 C_5 C_6 - C_1 C_{23} S_4 S_6 + C_1 S_{23} S_5 C_6 + S_1 S_4 C_5 C_6 + S_1 C_4 S_6$$

$$R_{21} = S_1 C_{23} C_4 C_5 C_6 - S_1 C_{23} S_4 S_6 + C_1 S_{23} S_5 C_6 - C_1 S_4 C_5 C_6 - C_1 C_4 S_6$$

$$R_{31} = -S_{23} C_4 C_5 C_6 + S_{23} S_4 S_6 + C_{23} S_5 C_6$$

$$R_{12} = -C_1 C_{23} C_4 C_5 S_6 - C_1 C_{23} S_4 C_6 - C_1 S_{23} S_5 S_6 - S_1 S_4 C_5 S_6 + S_1 C_4 C_6$$

$$R_{22} = -S_1 C_{23} C_4 C_5 S_6 - S_1 C_{23} S_4 C_6 - S_1 S_{23} S_5 S_6 + C_1 S_4 C_5 S_6 - C_1 C_4 C_6$$

$$R_{32} = S_{23} C_4 C_5 S_6 + S_{23} S_4 C_6 - C_{23} S_5 S_6$$

$$R_{13} = C_1 C_{23} C_4 S_5 - C_1 S_{23} C_5 + S_1 S_4 S_5$$

$$R_{23} = S_1 C_{23} C_4 S_5 - C_1 S_{23} C_5 - C_1 S_4 S_5$$

$$R_{33} = -S_{23} C_4 S_5 - C_{23} C_5$$

Solving for  $\theta_5$

From the above equations it may be observed that

$$(R_{13} C_1 + R_{23} S_1) S_{23} + R_{33} C_{23} = -C_5$$

Therefore,

$$\theta_5 = \pm \arccos\left(-\frac{(R_{13} C_1 + R_{23} S_1) S_{23} - R_{33} C_{23}}{C_5}\right)$$

Where the  $\pm$  signs specify the wrist-up and wrist-down solutions.

Solving for  $\theta_4$ , observe that

$$R_{23} C_1 - R_{13} S_1 = -S_4 S_5$$

and

$$(R_{13}C_1 + R_{23}S_1)C_{23} - R_{33}S_{23} = C_4S_4$$

Thus, when  $S_5 \neq 0$ , we can solve for  $\theta_4$  as

$$\theta_4 = \text{atan2}(-\text{sgn}(S_5))(R_{23}C_1 - R_{13}S_1), \text{sgn}(S_5)((R_{13}C_1 + R_{23}S_1)C_{23} - R_{33}S_{23}),$$

Where  $\text{atan2}(x)$  is the four-quadrant inverse tangent function, and  $\text{sgn}(x)$  is the sign of  $x$ . The case of  $S_5 = 0$  is a degenerate case with an infinite number of solutions for  $\theta_4$ . The only constraint is on the sum  $\theta_4 + \theta_6$ .

Solving for  $\theta_6$ , it may be verified that

$$R_{31}C_{23} + (R_{11}C_1 + R_{21}S_1)S_{23} = S_5C_6$$

and

$$R_{32}C_{23} + (R_{12}C_1 + R_{22}S_1)S_{23} = -S_5C_6$$

Thus when  $S_5 \neq 0$ , we can solve for  $\theta_6$  as

$$\theta_6 = \text{atan2}(-\text{sgn}(S_5))(R_{32}C_{23} + (R_{12}C_1 + R_{22}S_1)S_{23}),$$

$$\text{sgn}(S_5)R_{32}C_{23} + (R_{12}C_1 + R_{22}S_1)S_{23}),$$

Again, the degenerate case of  $S_5 = 0$  can be handled separately.

#### 4. CONCLUSIONS

It is generally recognized that the inverse kinematics problem is characterized with more difficulties than the forward kinematics problem. This is because of the multitude of solutions provided by the analytical method. The user then has the difficult task of zeroing in on the appropriate solution. The geometrical method of solution is simpler than the analytical method in this regard. Unfortunately the geometrical method can be used to find the inverse solution of only the very simple of robots.

The equation given by

$$P^{wrist} = P - d_n r^3$$

was applied during the current study to find the inverse kinematics solution for the first three joints. This equation permits the partitioning of the solution into two parts, one from the tool tip to the wrist, and the other from the wrist to the base. Consequently it was possible to

obtain expressions for  $P_X$ ,  $P_Y$ , and  $P_Z$  representing the wrist position. From these equations, the solutions of joints one, two, and three were derived. The solutions of the last three joints were derived from the orientation equations.

The utility of determination of relationships for the forward and inverse kinematics of robots becomes essential for a given type of robot when it is desired to program the robot. Thus the development of a teaching pendant relies on the availability of such relationships for the robot under consideration. The authors will present the development of such a robot motion simulation program for five types of robots elsewhere [Balamesh, et al., 2002].

## REFERENCES

1. Al-Matrafi, T.D., 2000, "Kinematic Simulation of a Six-Axis Robot Manipulator," Unpublished MS Thesis, King Abdulaziz Univ., Mechanical Eng. Dept., Jeddah 21589.
2. Balamesh, A. S., T.D. Almatrafi, A.A.N. Aljawi and M. Akyurt, 2002, "RobSim - a simulator for robotic motion", *Sixth Saudi Engineering Conf., KFUPM* (accepted).
3. Dehlawi, F.M., M. Akyurt, A.A. Aljawi, A.S. Balamesh and A.M. Al-Qasimi, 1996, "Design and Implementation of an industrial robot", Progress Report 2, KACST Project 12-42, Riyadh.
4. Denavit, J. and R.S. Hartenberg, 1955, "A Kinematic Notation for Lower Pair Mechanisms Based on Matrices," *J. Applied Mechanics*, 77, pp 215-221.
5. Fu, K.S., R.C. Gonzales and C.S.G Lee, 1987, *Robotics: Control, Sensing, Vision And Intelligence*, McGraw-Hill.
6. Lee, C.S.G. and M. Ziegler, 1983, "A geometric approach in solving the inverse kinematic of puma robots," *Proc. of the 13th Int Sym on Industrial Robots*, pp. 1601-16,18.
7. Paul, R., 1981, *Robot Manipulators: Mathematics, Programming and Control*, The MIT Press.
8. Pieper, D.L., 1968, "The Kinematics Of Manipulators Under Computer Control," Computer Science Department, Stanford University, Artificial Intelligence Project Mem. No. 72.
9. Schilling, R. J. , 1990, *Fundamentals of Robotics, Analysis and Control*, Prentice-Hall, Inc.
10. Uicker, J. J, J. Denavit, and R. S. Hartenberg, 1964, "Iterative Methods for Displacement Analysis of Spatial Mechanisms," *Trans ASME J. App Mech*, 31, Series E, pp 309-314.
11. Yang, A. T. and S. R. Frnden, 1964, "Application of Dual Number Quaternion Algebra to the Analysis of Spatial Mechanisms," *Trans ASME, J Appl Mech*, 31, pp 101-109.